J|A|C|S
ARTICLES

Published on Web 11/16/2009

# Amphiphillic Organic Crystals

J. J. Segura,[†] A. Verdaguer,[†] M. Cobián,[‡] E. R. Hernández,*[,‡] and J. Fraxedas*[,†]

*Centre d'Investigació en Nanociència i Nanotecnologia, CIN2 (CSIC-ICN), Edifici CM7, Esfera UAB, Campus de Bellaterra, E-08193 Barcelona, Spain, and Institut de Ciència de Materials de Barcelona ICMAB (CSIC), Campus de Bellaterra, E-08193 Barcelona, Spain*

Received July 17, 2009; E-mail: ehe@icmab.es; jordi.fraxedas@cin2.es

***Abstract:*** The amphiphillic character, that is, the capacity to simultaneously attract and repel water, has been traditionally reserved to organic molecules such as phospholipids and surfactants, containing both hydrophilic and hydrophobic groups within the same molecule. However, this general concept can be extended to artificial structures such as micrometer-sized particles, the so-called Janus particles, and patterned surfaces. Here we provide an example of an amphiphillic crystalline solid, L-alanine, by combining atomic force microscopy measurements performed on two different cleavage surfaces showing contrasting behaviors when exposed to water vapor, with computer simulations that allow us to clarify the dipolar origin of this behavior. Although we take L-alanine as an example, our results should apply quite generally to dipolar molecular crystals.

## 1. Introduction

Molecular amphiphillicity, the ability shown by a particular family of molecules to simultaneously exhibit high and low affinity to water, is a property of paramount importance in many fundamental and applied fields. Aside from its relevance to numerous practical issues of great economical impact, such as detergents, we draw our attention toward the key role that amphiphillic molecules have in biological systems. Water, the solvent medium of most biological assemblies, induces the self-assembly of such molecules in closed boundaries such as micelles and vesicles because of the dual hydrophilic and hydrophobic character of the molecules. This fundamental property is the basis of the widely used Langmuir−Blodgett technique, the earliest example of man-made supramolecular assembly.[1,2] According to a particular theory on the origin of life, known as *compartmentalistic*, the combination of water and amphiphillic molecules has played an essential role, in that the confinement of molecules within vesicles enabled prebiotic metabolic pathways.[3] These ideas are by no means universally accepted, but they highlight the relevance of the interfaces that water forms with molecular species, a view nowadays increasingly accepted.[4,5] Another matter of debate is the influence of the structuring of water layers on phospholipid membranes, which may hinder the transport and diffusion of molecules into the cells through such membranes.[6] The interplay between proteins and their water shell is also intensively studied. Increasingly, biochemistry regards proteins as complex structures that incorporate the shell of water surrounding them as an active component.[7] The bound water molecules are used as functional units, interacting with other proteins and substrates or transporting protons along the protein.[8−13] Many studies, both from the experimental and theoretical points of view, have sought to understand the complex role of water in protein biochemistry, but frequently, the lack of fundamental information about the interaction of water with each part of the protein makes their interpretation difficult or restricted to specific cases.[14−16]

The buildings blocks of proteins are α-amino acids, small organic molecules containing both a positively charged ammonium group ($NH_3^+$) and a negatively charged carboxylic group ($COO^-$), linked to a common carbon atom and to an organic substituent, also called radical. This charged configuration is known as the zwitterionic form of the amino acid and is the dominant one in aqueous solution over a wide range of pH values, as well as in the crystalline state, which is at the origin of the surprisingly high stability of such crystals (e.g., high melting point of about 300 °C). The degree of hydrophilicity/hydrophobicity of amino acids is a rather ambiguous parameter

[†] Centre d'Investigació en Nanociència i Nanotecnologia.
[‡] Institut de Ciència de Materials de Barcelona ICMAB (CSIC).

(1) Langmuir, I. *J. Am. Chem. Soc.* **1917**, *39*, 1848–1906.
(2) Blodgett, K. B. *J. Am. Chem. Soc.* **1935**, *57*, 1007–1022.
(3) Luisi, P. L. *The Emergence of Life: from Chemical Origins to Synthetic Biology*; Cambridge University Press: Cambridge, U.K., 2006; Chapter 2.
(4) Milhaud, J. *Biochim. Biophys. Acta* **2004**, *1663*, 19–51.
(5) Ball, P. *Chem. Rev.* **2008**, *108*, 74–108.
(6) Higgins, M. J.; Polcik, M.; Fukuma, T.; Sader, J. E.; Nakayama, Y.; Jarvis, S. P. *Biophys. J.* **2006**, *91*, 2532–2542.
(7) Ebbinghaus, S.; Kim, S. J.; Heyden, M.; Yu, X.; Hengen, U.; Gruebele, M.; Leitner, D. M. *Proc. Natl. Acad. Sci. U.S.A.* **2007**, *104*, 20749–20752.
(8) Colombo, M. F.; Ran, D. C.; Parsegian, V. A. *Science* **1992**, *256*, 655–659.
(9) Svergun, D. I.; Richard, S.; Koch, M. H. J.; Sayers, Z.; Kuprin, S.; Zaccai, G. *Proc. Natl. Acad. Sci. U.S.A.* **1998**, *95*, 2267.
(10) Lo Conte, L.; Cothia, C.; Janin, J. *J. Mol. Biol.* **1999**, *285*, 2177–2198.
(11) Makarov, V.; Pettitt, B. M.; Feig, M. *Acc. Chem. Res.* **2002**, *35*, 376–384.
(12) Lin, J.; Balabin, I. A.; Beratan, D. N. *Science* **2005**, *310*, 1311–1313.
(13) Garczarek, F.; Gerwert, K. *Nature* **2006**, *439*, 109–112.
(14) Ketteler, G.; Ashby, P.; Mun, B. S.; Ratera, I.; Bluhm, H.; Kaseno, B.; Salmeron, M. *J. Phys.: Condens. Matter* **2008**, *20*, 184024.
(15) Russo, D.; Ollivier, J.; Teixeira, B. S. *Phys. Chem. Chem. Phys.* **2008**, *10*, 4968–4974.
(16) Born, B.; Joong Kim, S.; Ebbingshaus, S.; Gruebele, M.; Havenith, M. *Faraday Discuss.* **2009**, *141*, 161–173.

  

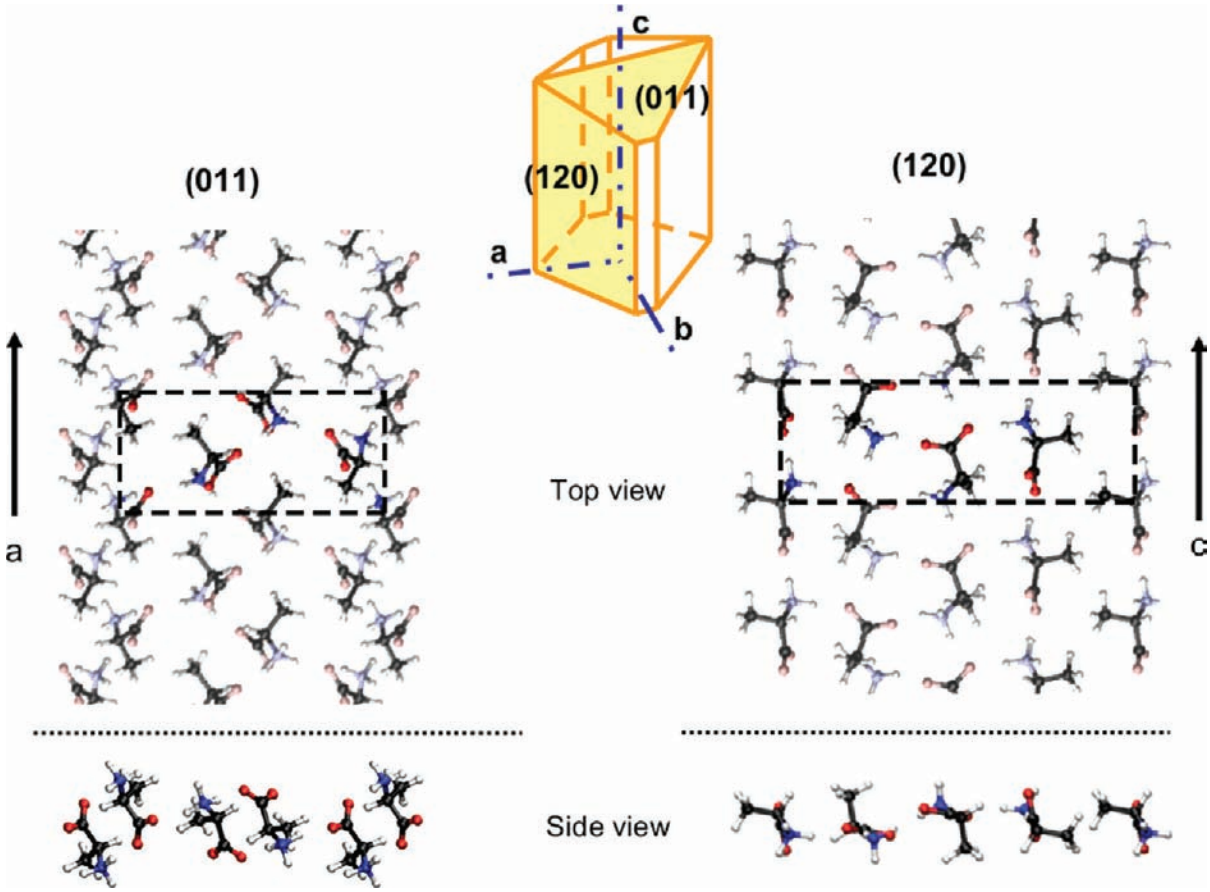


***Figure 1.*** Crystal habit and room temperature structure of L-alanine. The crystal structure is orthorhombic, space group $P2_12_12_1$, with four molecules per unit cell and cell parameters $a = 0.6032$, $b = 1.2343$ and $c = 0.5784$ nm. Crystallographic data taken from Lehmann and co-workers.[27] (Left) Top and side view of the (011) crystal face projected across (top) and along (below) the *a*-axis. Carbon, oxygen, nitrogen, and hydrogen atoms are represented by black, red, blue, and white spheres, respectively. (Right) Top and side view of the (120) crystal face projected across (top) and along (below) the *c*-axis.

and needs to be clarified.[17,18] Indeed, the hydrophilic character is ascribed to the charged groups, and the side chain contributes to the global topological hydrophilic/hydrophobic nature. Thus, the radical can be seen as a discrete variable parameter that contributes to the tuning of the general affinity to water.

In this work, we focus on L-alanine [(*S*)-2-aminopropanoic acid], one of the smallest amino acids, which has a nonreactive hydrophobic methyl group as side chain. In spite of being traditionally considered as a hydrophobic amino acid, it exhibits a relatively high solubility in water (16.65 g in 100 g of $H_2O$ at 25 °C) due to its zwitterionic form. The coexistence of the $NH_3^+$ and the $COO^-$ hydrophilic groups and the hydrophobic methyl group makes the hydration effects in L-alanine a rather complex phenomenon that has received considerable interest in recent years, mainly from the theoretical point of view.[19−22] We approach the problem of understanding the interaction of water with L-alanine by combining atomic force microscopy (AFM) measurements in ambient conditions[23] with molecular dynamics (MD) simulations of the model system water on (120) and (011) surfaces of single crystals. As will be shown below, both surfaces display contrasting behaviors when exposed to water vapor; namely, the (011) and (120) surfaces display hydrophilic and hydrophobic behavior, respectively. It is thus an interesting example of a material which exhibits amphiphillic character, complementing previous examples of patterned surfaces[24] and of colloidal (Janus) particles.[25,26] As will be discussed below, the crystalline order of the both surfaces greatly helps in the elucidation of the origin of the differentiated hydrophobic/hydrophilic character.

## 2. Crystal Structure of L-Alanine

Figure 1 shows a schematic view of the crystal habit of L-alanine indicating the *a*-, *b*-, and *c*-axes and the faces studied here, together with their projected room temperature crystal structures.[27] It has been argued[28] that the (120) surface of L-alanine is hydrophobic, and that this character is due to the

(17) Karplus, P. A. *Protein Sci.* **1997**, *6*, 1302–1307.
(18) Lienqueo, M. E.; Mahn, A.; Asenjo, J. A. *J. Chromatogr. A* **2002**, *978*, 71–79.
(19) Park, S.; Ahn, D.; Lee, S. *Chem. Phys. Lett.* **2003**, *371*, 74–79.
(20) Sagarik, K.; Dokmaisrijan, S. *J. Mol. Struct. (THEOCHEM)* **2005**, *718*, 31–47.
(21) Osted, A.; Kongsted, J.; Mikkelsen, K. V.; Christiansen, O. *Chem. Phys. Lett.* **2006**, *429*, 430–435.
(22) Degtyarenko, I.; Jalkanen, K. J.; Gurtovenko, A.; Nieminen, R. M. *J. Comput. Theor. Nanosci.* **2008**, *5*, 277–285.
(23) Verdaguer, A.; Sacha, G. M.; Bluhm, H.; Salmeron, M. *Chem. Rev.* **2006**, *106*, 1478–1510.
(24) Lenz, P.; Ajo-Franklin, C. M.; Boxer, S. G. *Langmuir* **2004**, *20*, 11092–11099.
(25) Jiang, S.; Granick, S. *Langmuir* **2008**, *24*, 2438–2445.
(26) Kim, J.-W.; Lee, D.; Shum, H. C.; Weitz, D. A. *Adv. Mater.* **2008**, *20*, 3239–3243.
(27) Lehmann, M. S.; Koetzle, T. F.; Hamilton, W. C. *J. Am. Chem. Soc.* **1972**, *94*, 2657–2660.

presence of exposed methyl groups on this surface; however, a quick inspection of the crystal structure along the *c*-axis (bottom right in Figure 1) reveals that only one molecule out of every four has its methyl group pointing outward on this surface, and that carboxylic and amino groups are also clearly exposed. Thus, the experimental evidence of low affinity to water in this surface is in contrast with the molecular distribution, hence our interest in this apparent contradiction. Likewise, both polar and nonpolar groups are present at the (011) surface (see bottom left in Figure 1). In conclusion, the prediction of the hydrophobic/hydrophilic character from the ideal molecular structure alone may lead, in certain cases, to erroneous results, so that other criteria are needed.[29]

## 3. Experimental and Computational Methods

**3.1. Experimental Details.** Single crystals of L-alanine were prepared by dissolving as-received commercial powder (Fluka, nominal purity ≥99.5%) in Milli-Q water. The alanine/water dissolution was heated to 40 °C and then cooled to room temperature with a temperature ramp of $-1.5 \times 10^{-3}$ °C/h, without any buffer solution. With this method, crystals with long dimensions spanning from 5 mm to 2 cm are obtained, which are largely sufficient for our AFM experiments. The room temperature cell parameters of selected single crystals obtained with X-ray diffraction were $a = 0.60304$ nm, $b = 1.23450$ nm, and $c = 0.57887$ nm [$P2_12_12_1$ space group], in agreement with previous neutron diffraction studies.[27]

AFM experiments were carried out at room temperature with a 5500 Agilent Technologies AFM (Agilent Technologies, Santa Clara, CA) under controlled humidity, using microfabricated silicon cantilevers with force constants $k_c \sim 45$ N m $^{-1}$ and ultrasharp silicon tips (tip radius $R \leq 10$ nm) (PPP-NCHR, NanoAndMore GmbH, Darmstadt, Germany). All experiments were performed in a glovebox. The relative humidity (RH) inside the box was controlled by flowing dry nitrogen in order to decrease RH or by bubbling nitrogen through Milli-Q water to increase RH. The single crystals were cleaved inside the glovebox at the lowest attained RH (<5%). The experimental error in RH is typically ±5%.[30]

**3.2. Computational Details.** We have used the CHARMM[31] parametrization to model the alanine and water molecules, as well as their mutual interaction. For a detailed description of this model, the reader should consult the original reference, but briefly, the CHARMM model includes harmonic springs to describe all pairs of covalently bonded atoms within a molecule; it also uses harmonic potentials to account for bond angles; dihedral angles are also described. Partial charges on the atoms are used to reproduce the dipole of the alanine and water molecules (average water dipole 2.6 D, average alanine dipole 15.1 D). Lennard-Jones-type potentials are used to describe the dispersion-type forces arising between pairs of atoms.

MD simulations have been carried out employing the DL-POLY[32] package. In this package, the electrostatic interactions are accounted for with the Ewald summation method. Simulations have been conducted within the microcanonical (constant number of particles, constant volume, and constant energy) ensemble, using a time step of 1 fs, which is sufficiently short to result in good energy conservation during the length of our simulations. Initial velocities were chosen randomly from the Maxwell−Boltzmann distribution at room temperature, and the system was allowed to equilibrate at this temperature at the start of each simulation. In the case of the (120) surface, we simulated a L-alanine slab consisting of an 8 × 3 surface supercell, having dimensions of 4.63 × 5.18 nm$^2$; for the case of the (011) surface, we employed an 8 × 4 supercell, with dimensions of 4.83 × 5.4 nm$^2$. The (120) slab contained a total of 1152 alanine molecules, while the (011) slab consisted of 1024. The total number of water molecules in the simulation box varied between a minimum of 7500 up to a maximum of 8800. The dimension of the simulation box perpendicular to the crystal slab was chosen so as to tune the conditions to ambient temperature and pressure (300 K, 1 atm) during an equilibration period previous to the production runs. We used values of 15.18 and 15.07 nm for the (120) and (011) surfaces, respectively. Initial configurations for the simulations were generated by placing a slab (exposing the desired surfaces) cut out of the perfect alanine crystal in the middle of the simulation box and placing the appropriate number of water molecules at random positions above and below the slab. We then simulated the combined system for several picoseconds while constraining the alanine molecules in their equilibrium positions, so as to allow the water molecules to equilibrate. Subsequently, all restraints were lifted, and the whole system was allowed to equilibrate for a subsequent period of time, previous to the production runs. For convenience of analysis and visualization, in some cases (as discussed in the text), we imposed restraints on the mobility of the alanine molecules, although the conclusions from our simulation work are extracted from simulations in which no constraints were imposed.

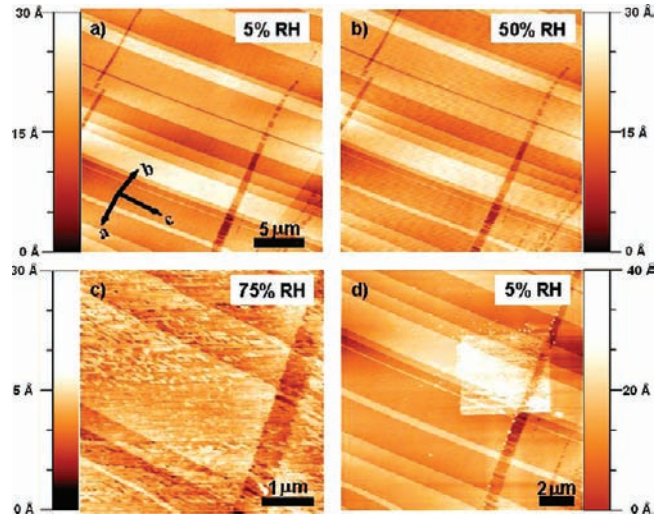


***Figure 2.*** Topographic AFM images of a (120) surface of a L-alanine single crystal. The images were acquired on freshly cleaved surfaces in the acoustic (tapping) operation mode in a glovebox at room temperature and at the relative humidities: (a) 5%, (b) 50%, (c) 75%, and (d) 5% after exposure to 75%. Cleavage was performed at RH <5%.

## 4. Results and Discussion

**4.1. Experimental Results.** Figure 2a shows a topographic AFM image obtained in acoustic (tapping) mode of a freshly cleaved (120) surface of a L-alanine single crystal measured at low RH (∼5%). The surface consists of micrometer-sized terraces separated by straight steps along the crystallographic [001] direction (*c*-axis), as determined by X-ray diffraction (see Figure 1, right). Identical results are obtained by cleaving either in air or at ∼5% RH. Previous AFM images taken in ambient conditions with molecular resolution of cleaved (120) surfaces

(28) Gavish, M.; Wang, J. L.; Eisenstein, M.; Lahav, M.; Leiserowitz, L. *Science* **1992**, *256*, 815–818.
(29) Partial AFM results performed in the same experimental setup under the same conditions on cleaved single crystals of L-valine and L-leucine show the same behavior as for the (120) surface of L-alanine, that is, negligible affinity. However, in this case, the bilayer structure of both systems, which is exposed to water surfaces made exclusively of methyl groups, makes the prediction of their hydrophobic character straightforward.
(30) Verdaguer, A.; Cardellach, M.; Fraxedas, J. *J. Chem. Phys.* **2008**, *129*, 174705-1–174705-7.
(31) MacKerell, A. D., Jr.; et al. *J. Phys. Chem. B* **1998**, *102*, 3586–3616.
(32) Smith, W.; Forester, T. *J. Mol. Graphics* **1996**, *14*, 136.

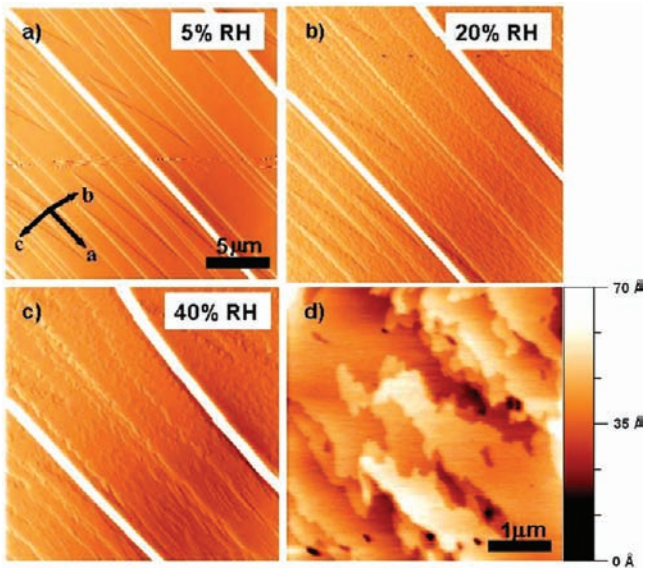


***Figure 3.*** Amplitude AFM images of a (011) surface of a L-alanine single crystal. The images were acquired on freshly cleaved surfaces in the acoustic (tapping) operation mode in a glovebox at room temperature and at the relative humidities: (a) 5%, (b) 20%, and (c) 40%. A zoom taken in the topographic mode at 40% RH is shown in (d).

show no reconstruction or relaxation; that is, the surface retains the ideal bulk structure.[33] Step heights are integer multiples of ≃0.5 nm, the distance between two adjacent (120) planes (0.519 nm). After slowly increasing RH up to ∼50% (Figure 2b), we observe that the surface remains unchanged. A further increase up to ∼75% shows important morphological changes, although the original stepped structure can still be observed (Figure 2c). In order to determine tip-induced effects at such high humidity, RH was decreased again down to ∼5% and a larger area was then scanned (Figure 2d). The area that was not scanned at high humidity appears unperturbed, indicating the negligible affinity of the (120) surface to water even at elevated RHs. Modifications induced by the tip are due to the formation of a tip−sample liquid water neck.[34,35]

The (011) surfaces of L-alanine single crystals have been explored using the same methodology as for the (120) surfaces. Freshly cleaved surfaces at low humidity show terraces with triangular steps (Figure 3a), with a preferential step direction along the [100] direction (*a*-axis), as indicated in the figure. The direction of the arrow-shaped steps (angles between 5 and 30°) corresponds to the direction of the crack propagation.[36] The measured step height is again ≃0.5 nm, corresponding to the distance between two adjacent (011) planes. Contrary to what is observed in the (120) surfaces, irreversible roughening of the terraces is observed at the lowest achieved RHs. In fact, roughening is already observed at the first image taken after cleavage at RH ∼5%, a clear proof of its affinity to water. When RH is slowly increased, dramatic changes are observed and already at RH <20% terraces and steps appear strongly perturbed (Figure 3b), and at 40% RH, steps are hardly recognizable (Figure 3c). A detail of a terrace (Figure 3d) shows the strong perturbation caused by water. Indeed, for increasing RH values, the perturbation induced by the tip becomes more relevant. However, surface roughening induced by water is observed in regions of the surface that were not previously scanned, following the same strategy described above for the (120) surface (see Supporting Information).

**4.2. Simulation Results.** In order to understand the microscopic origin of the different behaviors observed in our experiments, we carried out a series of simulations of alanine crystals cut so as to expose either the (120) or (011) surface, which were then placed in contact with bulk water. In Figure 4a, we plot the density profile (integrated over planes parallel to the surface) of water molecules as a function of the height above the surface, for both the (011) and (120) surfaces, as well as the spatial distribution of this density. The probability densities have been calculated with the positions of the center of mass of the water molecules. The distance origin is somewhat arbitrary, given that the topographies of the two surfaces are different. A common origin for the various curves is set by overlapping the distribution of atoms belonging to the surface alanine molecules and setting the zero mark at the point where these distributions fall down to zero. The peaks appearing in Figure 4a measure approximate distances to the plane of outermost atoms of the alanine crystal surface. The fact that in some cases the distributions take finite values at negative height is indicative of a degree of penetration of the water molecules into the alanine crystal surfaces, due to the rugosity of the latter. As can be seen in the figure, the density profiles of water on both surfaces at distances smaller than 8 Å are markedly different, with water molecules getting much closer to the outer alanine molecules in the case of the (011) surface than in the (120). In fact, in the case of the (011) surface, there is a first peak centered at zero, which reveals the presence of water molecules in close contact to the surface. This peak corresponds to hydrogen bond formation between water molecules and surface carboxyl groups mediated by a proton from the water molecule participating in the bond, as well as between the amino groups and water molecules, mediated by a proton from the amino group. No similar peak is found for the (120) surface, where the distribution has a first peak at a position of ≈1.8 Å from the surface. Although there is also some degree of hydrogen bond formation between water and alanine groups on this surface, it does not happen to the extent it does on the (011) surface. These different patterns confirm the relative hydrophilic/hydrophobic character of the (011) and (120) surfaces, respectively. The positions of the distribution peaks shown in Figure 4a correspond to typical hydrogen bond distances that are established between water and alanine molecules at the surface. Our results are in line with the accepted view that water molecules move away from extended hydrophobic surfaces forming a depleted density region near such a surface.[37−42]

(33) Guo, H. M.; Liu, H. W.; Wang, Y. L.; Gao, H. J.; Gong, Y.; Jiang, H. Y.; Wang, W. Q. *Surf. Sci.* **2004**, *552*, 70–76.
(34) Sacha, G. M.; Verdaguer, A.; Salmeron, M. *J. Phys. Chem.* **2006**, *110*, 14870–14873.
(35) Contact-angle measurements carried out with several single crystals lead to non-conclusive results. The values obtained for the (120) surface are rather small (≤30°), well below the accepted values for hydrophobic surfaces. The reason for these low values lies in the stepped nature of the cleaved surfaces; water adheres to the steps, as made evident by phase AFM images.
(36) Engelhardt, J. B.; Dabringhaus, H.; Wandelt, K. *Surf. Sci.* **2000**, *448*, 187–200.
(37) Stillinger, F. H. *J. Solution Chem.* **1973**, *2*, 141–158.
(38) Lum, K.; Chandler, D.; Weeks, J. D. *J. Phys. Chem. B* **1999**, *103*, 4570–4577.
(39) Chandler, D. *Nature* **2005**, *437*, 640–647.
(40) Jensen, M. O.; Mouritsen, O.-G.; Peters, G. H. *J. Chem. Phys.* **2004**, *120*, 9729–9744.
(41) Poynor, A.; Homg, L.; Robinson, I. K.; Granick, S.; Zhang, Z.; Fenter, P. A. *Phys. Rev. Lett.* **2006**, *97*, 266101.

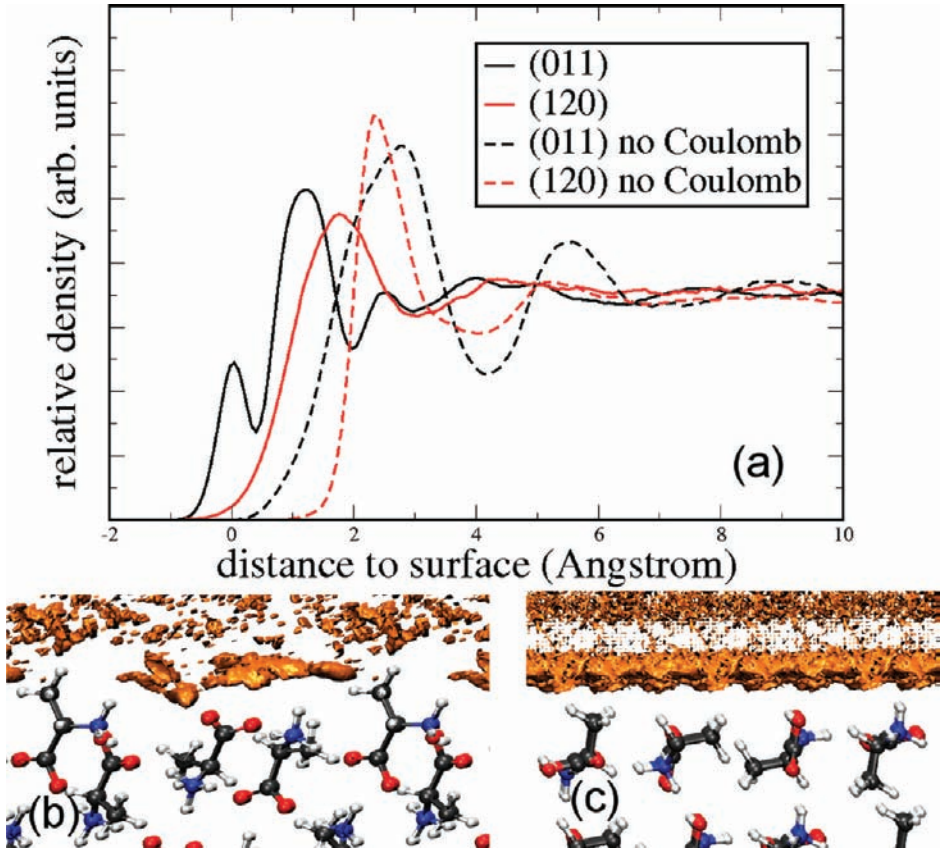


***Figure 4.*** Distribution of water molecules on L-alanine surfaces. (a) Probability density of water molecules above surfaces (011) (black) and (120) (red) of alanine, obtained from MD simulations. Continuous lines show water probability densities calculated with water/alanine charges switched on and including the dynamics of the alanine molecules, while the dashed lines are the resulting densities obtained without water/alanine electrostatic interactions and fixing the alanine molecules at perfect crystal positions. The lower panels show the spatial distribution of the nearest water molecules on L-alanine crystal surfaces; (b) (011) surface viewed along the *a*-axis; note that during the MD simulations the (011) surface reconstructs slightly (compare with Figure 1); (c) (120) surface viewed along the *c*-axis. No appreciable reconstruction is observed in this case.

To uncover the reasons behind these different patterns, we have repeated the same simulations, but turning off the electrostatic interactions between the alanine and water molecules, by setting the partial charges on alanine constituent atoms to zero. Since neglecting the contribution of the electrostatic interactions would significantly change the structure of the alanine crystal, in these simulations, we have frozen the alanine molecules at their perfect crystal positions and only considered the dynamics of the water molecules. The resulting densities from this second set of simulations are shown in Figure 4a as dashed lines. As can be seen by comparing the distributions obtained with and without electrostatic interactions, these play a crucial role in determining the distribution of water molecules on the (011) surface but are of lesser importance in the case of the (120) surface. Indeed, without electrostatic interactions, the density profile of water on alanine (011) changes dramatically, losing all of the structure present when alanine atomic charges are considered. In particular, the short distance peak disappears, and the density takes its first maximum at roughly the same position as in the case of the (120) surface (also without Coulomb interactions). In contrast, in the case of the latter surface, the exclusion of the electrostatic interactions does not change quite so radically the form of the water density profile; it only results in an approximately rigid shift toward longer distances and a slight narrowing of the features already present in the distribution when alanine charges are turned on. The overall effect of the electrostatic interactions in this case is to bind the water molecules slightly more strongly to the (120) surface, but the actual shape of the distribution is determined by the dispersion-type interactions, the only ones present between substrate and water when alanine charges are not included.

Our results are in line with recent MD simulations of bulk water in contact with extended hydrophobic and hydrophilic crystalline surfaces of *n*-alkane $C_{36}H_{74}$ and *n*-alcohol $C_{35}H_{71}OH$, respectively,[40] and with neutron reflectivity experiments conducted on self-assembled monolayers in water.[43] However, a notable difference between previous results and those reported here is that hitherto either the substrate[40] or the solvent[43] were changed (from polar to nonpolar) to observe a change in the hydrophilic/hydrophobic character. Here, in contrast, it is the same material that is displaying two markedly different behaviors. Since one normally associates hydrophobicity with nonpolar materials, and at the same time expects polar ones to be hydrophilic, it remains to be explained how can a polar material such as the L-alanine molecular crystal display both characters, depending on the exposed surface.

(42) Mezger, M.; Reichert, H.; Schöder, S.; Okasinski, J.; Schröder, H.; Dosch, H.; Palms, D.; Ralston, J.; Honkimäki, V. *Proc. Natl. Acad. Sci. U.S.A.* **2006**, *103*, 18401–18404.

(43) Maccarini, M.; Steitz, R.; Himmelhaus, M.; Fick, J.; Tatur, S.; Wolff, M.; Grunze, M.; Janecek, J.; Netz, R. R. *Langmuir* **2007**, *23*, 598–608.

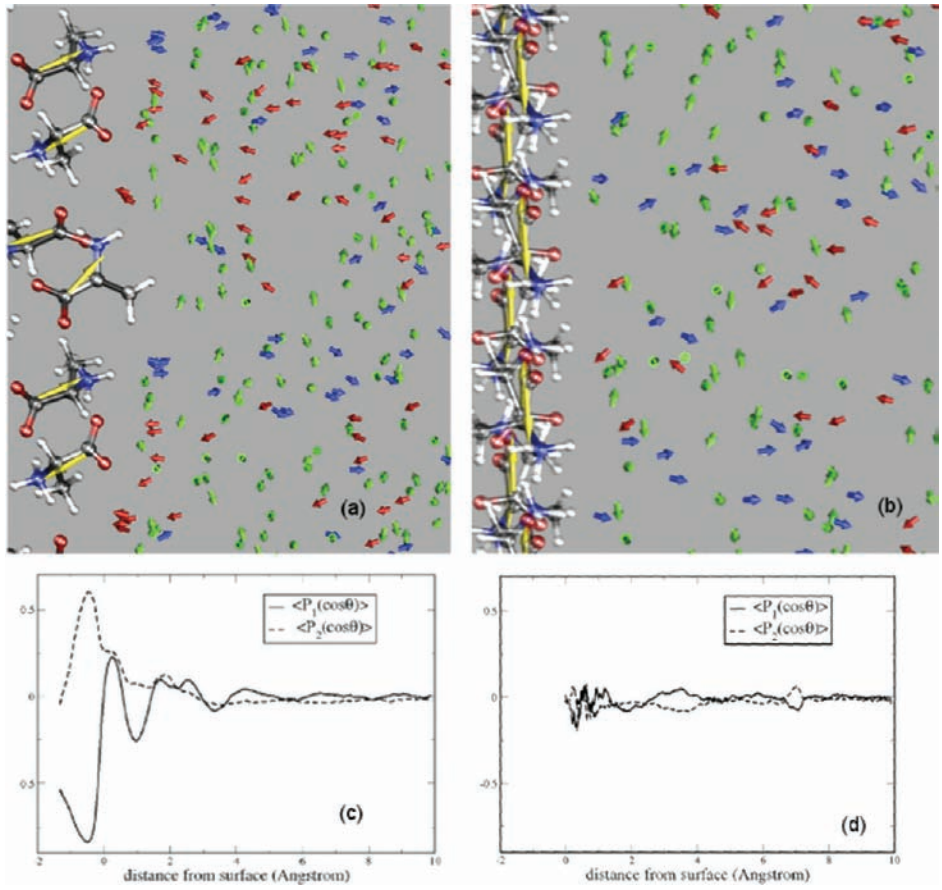


***Figure 5.*** Distribution of molecular dipoles at L-alanine/water interfaces. Instantaneous configurations of the dipoles of water molecules resulting from simulations of the (011) (a) and (120) (b) surfaces exposed to water. Alanine molecular dipoles are shown in yellow, superimposed on the corresponding molecules. The average value of the alanine dipole obtained in our simulations is 15.1 D. Water molecular dipoles are shown in a color code, where blue indicates dipoles pointing away from the interface ($\cos\theta \geq 0.5$, where $\theta$ is the angle between the molecular dipole and the outward pointing surface normal), red indicates dipoles pointing toward the interface ($\cos\theta \leq -0.5$), and green indicates dipoles lying roughly parallel to the surface ($-0.25 \leq \cos\theta \leq 0.25$). In order to highlight the orientation of the water molecular dipoles, the water molecules themselves are not shown. The average value of water molecular dipoles obtained in our simulations is 2.6 D. (c,d) Functions $\langle P_1(\cos\theta)\rangle$ and $\langle P_2(\cos\theta)\rangle$ calculated as a function of distance along the surface normal, for the (011) and (120) surfaces, respectively.

Figure 4 conforms to the view that corrugated surfaces have a tendency to be more hydrophilic than flat or featureless ones. The presence of asperities in the former allows water molecules to arrange themselves in such a way as to minimize the disruption to the hydrogen bond network in water close to the surface; the impossibility to do this in the proximity of featureless surfaces leads, in contrast, to dewetting.[38,39] Indeed, Figure 4b shows that the (011) surface is more highly corrugated than the (120) one. This, in turn, leads to a more irregular pattern in the distribution of water molecules in the proximity of the (011) surface, with some regions having water molecules going into cavities or voids in the surface. In contrast, the distribution of water molecules in the proximity of the (120) surface is comparatively featureless (see Figure 4c), with no close contacts between alanine and water molecules. The presence of an increased water density (with respect to the liquid bulk) close to the (120) surface that can be seen in Figure 4a is not incompatible with the hydrophobic character of the surface.[39,44]

At first sight, it is natural to assume that the contrast in the observed behavior of water on the (011) and (120) surfaces is due to the different disposition of the polar groups of the alanine moieties in each of these surfaces. Such arguments, however, do not lead to a clear criterion for determining the hydrophobic/hydrophilic character of a given surface. Indeed, they may even lead to error; noticing the presence of methyl chemical groups in the (011) surface (see Figure 4b), one may easily conclude that this surface should be hydrophobic when in fact it is not. A much more revealing observation is obtained by focusing not on the disposition of the different chemical groups on the exposed surfaces but rather on the orientation of the molecular dipoles. In Figure 5, we display two snapshots obtained from simulations of the (011) (left) and (120) (right) surfaces exposed to bulk water. The first striking observation to be extracted from Figure 5 is the different disposition of the alanine dipoles (shown as yellow arrows) seen in both surfaces. While in the case of the (011) surface the alanine dipoles are arranged in such a way as to form angles of roughly 45 and 135° with the surface normal, in the (120) surface, they are contained within the plane of the surface. The second key observation is that the orientation of the alanine dipoles in the two surfaces induces a radically different distribution of dipole orientations in the nearby water molecules. On the (011) surface, water molecules close to the surface orient themselves with their dipoles either pointing out (blue color) or in (red), depending on whether the dipole of the nearest alanine molecule is pointing out of or into the crystal, as this optimizes the dipole−dipole interaction energy; green

(44) Mittal, J.; Hummer, G. *Proc. Natl. Acad. Sci. U.S.A.* **2008**, *105*, 20130–20135.

arrows are for water molecules with dipoles oriented roughly parallel to the surface. This can be clearly seen in Figure 5a, where there is a predominance of red (blue) arrows at the points where the surface alanine dipoles are pointing in (out) from the surface, with only a minority of green arrows. In the case of the (120) surface (see Figure 5b), the situation is different: no clear preference for any given orientation of the water dipoles can be discerned, and all orientations can be observed. Although panels a and b of Figure 5 show instantaneous configurations of the water dipoles in the proximity of the (011) and (120) surfaces, the differences revealed by these images are actually maintained in average over time, as shown in panels c and d. There, we plot two functions, $\langle P_1(\cos\theta)\rangle$ and $\langle P_2(\cos\theta)\rangle$, where $P_1$ and $P_2$ are the first- and second-order Legendre polynomials, defined as $P_1(x) = x$ and $P_2(x) = 1/2(3x^2 - 1)$, respectively, $\theta$ is the angle formed by the dipole of a water molecule with the outward pointing surface normal, and the angular brackets indicate an average over water molecules and over configurations produced during the simulation. $P_1$ provides information about the average orientation of the water dipoles, while $P_2$ allows one to distinguish between two possible cases leading to the same value of $P_1$, namely, the case of anisotropic orientation of dipoles ($P_1 = 0, P_2 = 0$) and the case of orthogonal orientation to the surface normal ($P_1 = 0, P_2 = -1/2$). It is apparent that the arrangement and orientation of water molecules is significantly different in both cases. Considering first the (011) surface, we see that $\langle P_1\rangle$ takes negative values at short distances, consistent with the fact that the nearest water molecules have their dipoles oriented antiparallel (red) to the surface normal. As the distance to the surface is increased, there is some oscillation from negative to positive values, reflecting local domains of slight predominance of antiparallel/parallel orientation of the water dipoles to the surface normal, decaying to zero further away from the surface. The decay of $\langle P_1\rangle$ to zero, and that of $\langle P_2\rangle$, is indicative of a transition from highly oriented dipolar arrangements close to the surface toward a situation of randomly oriented dipoles as we move into the liquid bulk. In contrast, the values of $\langle P_1\rangle$ and $\langle P_2\rangle$ on the (120) surface are always close to zero, regardless of the distance to the surface; clearly, in this case, interaction with the surface is not strong enough to induce any favored orientation of the water molecular dipoles.

Thus it can be seen that the orientation of the alanine molecular dipoles is the key to the hydrophobic/hydrophilic nature of the alanine surfaces. This is clear if we take into account that the electrostatic interaction between two dipoles, $\boldsymbol{\mu}_a$ and $\boldsymbol{\mu}_b$, separated by a distance $r_{ab}$ is given by

$$E_{dd} = \frac{1}{r_{ab}^3}[\boldsymbol{\mu}_a\cdot\boldsymbol{\mu}_b - 3(\boldsymbol{\mu}_a\cdot\hat{\mathbf{r}}_{ab})(\boldsymbol{\mu}_b\cdot\hat{\mathbf{r}}_{ab})] \quad (1)$$

where $\hat{\mathbf{r}}_{ab}$ is the normalized vector in the direction from $a$ to $b$. When two dipoles, separated by a distance $r_{ab}$, are in a colinear orientation, their interaction is twice as favorable as when they are in an antiparallel orientation at the same distance. The most favorable orientation that the water molecules can adopt above the (120) alanine surface is such that their molecular dipole is oriented antiparallel to that of the nearest alanine surface molecule. Since on this surface the alanine molecules are placed such that their dipoles are contained in the plane of the surface, the nearby water molecules cannot orient themselves in a more favorable way than this. However, in the case of the (011) surface, it is possible for the water molecules to orient themselves such that their dipoles are nearly colinear with that of the nearest alanine surface molecule, leading to a more strongly favorable interaction. Taking these considerations into account, it is now easy to explain the observations reported in Figure 4 concerning the effects on the distribution of water molecules when switching off the electrostatic interactions between alanine and water molecules, where it was seen that the electrostatic interactions had a much more noticeable effect in the case of the (011) surface and a very small one for the (120) surface. Analyzing our simulation trajectories, we find that water molecules tend to form hydrogen bonds with the (011) surface more readily than they do in the case of the (120) surface. This is consistent with the hydrophilic character of the first surface and the hydrophobic one of the latter.

**4.3. Concluding Remaks.** The amphiphillic character of single crystals of the amino acid L-alanine has been studied by combining AFM measurements with MD calculations. The underlying mechanism of the differentiated affinity of molecular surfaces to water is the dipolar distribution of the surface molecules. While dipoles pointing perpendicularly to the surface plane induce the structuring of water at short distances, dipoles parallel to the surface plane have little effect on water molecules, a text book example of electrostatic interaction between dipoles.

Although our findings apply to the particular case of L-alanine, they should be of wider applicability to other dipolar molecular solids and may be of relevance for understanding the complex interplay of biomolecules, such as proteins, with water, that is, protein hydration, essential for their three-dimensional structure and activity. The rationalization of the physicochemical processes governing the interaction of water with molecules and extended surfaces should ultimately provide the basis for the future design of intelligent surfaces with desired response to water.[45]

**Acknowledgment.** This work was supported by the Ministerio de Ciencia y Tecnología (Spain), through project FIS2006-12117-C04-01 and by the Generalitat de Catalunya (SGR 00909 and SGR 683). J.J.S. and M.C. thank the Consejo Superior de Investigaciones Científicas (CSIC) for a JAE DOC Ph.D. grant and a I3P postdoctoral fellowship, respectively, and A.V. acknowledges support from the Spanish Ramón y Cajal Program. Thanks are due to J. Santiso and E. Molins for the X-ray diffraction measurements of single crystals, and to J. Veintemillas for his valuable comments on the growth of the single crystals.

**Supporting Information Available:** Topography and phase AFM images of a (011) surface evidencing the influence of the scanning tip. Distribution of distances between surface alanine polar group atoms and water atoms on the (011) and (120) surfaces. This material is available free of charge via the Internet at http://pubs.acs.org.

JA905961H

(45) Nagase, K.; Kobayashi, J.; Okano, T. *J. R. Soc. Interface* **2009**, *6*, S293–S309.